Structure of CT26 in the C-terminal of Amyloid Precursor Protein Studied by NMR Spectroscopy

Dong-Il Kang, Dongha Baek, Song Yub Shin,† and Yangmee Kim*

Department of Chemistry and Bio/Materials Informatics Center, Konkuk University, Seoul 143-701, Korea
**E-mail: ymkim@konkuk.ac.kr*
†Department of Bio-Materials, Graduate School and Research Center for Proteineous Materials, Chosun University, Gwangju 501-759, Korea
Received June 7, 2005

C-terminal fragments of APP (APP-CTs), that contain Aβ sequence, are found in neurotic plaques, neurofibrillary tangles and the cytosol of lymphoblastoid cells obtained from AD patients. CT26, Thr639-Asp664 (TVIVITLVMLKKKQYTSIHH GVVEVD) includes not only the transmembrane domain but also the cytoplasmic domain of APP. This sequence is produced from cleavage of APP by caspase and γ-secretase. In this study, the solution structure of CT26 was investigated using NMR spectroscopy and circular dichroism (CD) spectropolarimeter in various membrane-mimicking environments. According to CD spectra and the tertiary structure of CT26 determined in TFE-containing aqueous solution, CT26 has an α-helical structure from Val^2 to Lys^{11} in TFE-containing aqueous solution. However, according to CD data, CT26 adopts a β-sheet structure in the SDS micelles and DPC micelles. This result implies that CT26 may have a conformational transition between α-helix and β-sheet structure. This study may provide an insight into the conformational basis of the pathological activity of the C-terminal fragments of APP in the model membrane.

Key Words : Alzheimer's disease, APP, CT26, NMR spectroscopy, CD spectroscopy

Introduction

Alzheimer's disease (AD) is the most common causative brain disease of primary dementia in the elderly. The most characteristic change in progressive dementia of Alzheimer's type is a tissue deposit of amyloid beta peptide, which is derived from its precursor protein APP.[1-12] Mutations in the beta-amyloid precursor protein (APP) gene cause familial Alzheimer's disease (AD). Although amyloid beta peptide (Aβ) is the principal constituent of senile plaques in AD, other cleavage products of APP are also implicated in playing roles in the pathogenesis of AD. C-terminal fragments of APP (APP-CTs) are found in neuritic plaques, neurofibrillary tangles and the cytosol of lymphoblastoid cells obtained from AD patients. Structural alterations of APP are implicated in the pathogenesis of Alzheimer's disease, but it is not known how they cause the disease. The amyloid precursor protein presents several cleavage sites leading to the release of its entire C-terminal domain into the cytoplasm. During apoptosis, this C-terminal domain can be cleaved at amino acid 664 by caspases 3, 6, and 8 and can thus generate a peptide, CT26.[10-12] Cytoplasmic APP sequence, Lys649-Asp664 (CT16) has been known as the most toxic part in the C-terminal of APP. CT26, Thr639-Asp664 (TVIVITLV MLKKKQYTSIHHGVVEVD) has not only the cytoplasmic toxic domain (CT16) but also the transmembrane domain.[13]

In order to understand the conformational basis of the pathological activity of the C-terminal fragments of APP, the structure of CT26 has been studied. Here, we studied the structures of CT26 using CD and NMR spectroscopy in membrane mimetic environments.

Experimental Section

Sample Preparation. Peptide CT26 was synthesized on Rink Amide MBHA resin as C-terminal amides by the solid phase method using Fmoc-chemistry, and was purified by a preparative reverse-phase C_{18} column. Trifluoroethanol (TFE) was purchased from ALDRICH Chemical Co. and perdeuterated sodium dodecyl sulfate (SDS-d_{25}) was obtained from Cambridge Isotope Inc. For NMR experiments, peptide was dissolved in 0.45 mL of TFE/H_2O (1 : 1, v/v) to make a final concentration of 1.0 mM.

CD Experiments. CD measurements of 100 μM peptide solutions were performed on a J720 spectropolarimeter (Japan, Jasco) between 190 and 250 nm at 298 K using quartz cell having pathlength of 1 mm. Data were collected at 0.1 nm-interval and 10 scans were averaged with the scan rate of 100 nm/min. In order to investigate the conformations in membrane-mimicking environment, peptides were dissolved in 30%-70% (v/v) TFE-containing aqueous solution, SDS micelles, and DPC micelles.

NMR Spectroscopy. Samples for NMR experiments were dissolved in 50% TFE/H_2O (1 : 1, v/v) solution. CT26 in SDS and/or DPC micelle were too poorly behaved in solution to be amenable to structure determination. CT26 were aggregated in both micelles at 1 mM concentration. All of the phase-sensitive two-dimensional experiments, such as DQF-COSY, TOCSY, and NOESY were performed using time-proportional phase incrementation method.[14-18] TOCSY experiments were performed using 80 ms MLEV-17 spin-lock mixing pulses. Mixing times of 150 ms and 250 ms were used for NOESY experiments. $^3J_{HN\alpha}$ coupling con-

stants were measured from DQF-COSY spectrum with a spectral width of 4006.41 Hz and digital resolution of 0.98 Hz/point.[19] All NMR spectra were recorded at 298 K on Bruker 400 MHz DPX-spectrometer at Konkuk University and on Bruker 500 MHz spectrometer at KBSI and processed off-line using the FELIX software (Molecular Simulations Inc., San Diego, CA, USA) on SGI workstation in our laboratory.

Structure Calculation. Distance constraints were extracted from the NOESY spectra with mixing times of 250 ms. All the NOE intensities were divided into three classes, strong, medium, and weak with the distance ranges of 1.8-2.7, 1.8-3.5, and 1.8-5.0 Å, respectively.[20,21] Structure calculations were carried out using X-PLOR version 3.851.[22] Standard pseudoatom corrections were applied to the nonstereospecifically assigned restraints,[23] and the additional 0.5 Å was added to the upper bounds for NOEs involving methyl protons.[24] Standard distance geometry-dynamical simulated annealing hybrid protocol was employed to generate structures.[25,26] The target function that is minimized during simulated annealing comprised only quadratic harmonic potential terms for covalent geometry, square-well quadratic potentials for the experimental distance and torsion angle restraints, and a quartic van der Waals repulsion term for the nonbonded contacts. Total of 80 structures were generated, 20 structures with the lowest energies were selected for the further analysis.

Results and Discussion

Circular Dichroism Study. To investigate the secondary structure of CT26 in membrane mimetic environments, CD spectra were measured in aqueous buffer, TFE/water solution, SDS micelles, and DPC micelles. As shown in Figure 1, CT26 has a random coil structure in water. Addition of TFE induces structural changes of CT26 and adopts α-helical conformation. CT26 in SDS micelles and DPC micelles show β-sheet structure.

Resonance Assignment and Secondary Structure. In order to investigate the tertiary structure of CT26 and to understand the changes induced by TFE, tertiary structure of CT26 in TFE/water solution was determined by NMR spectroscopy. Standard sequential assignment strategy was applied using DQF-COSY, TOCSY and NOESY spectra. Figure 2 shows NOESY spectrum with the assignments of CT26 in the NH-NH region. Table 1 lists the complete assignments of the proton chemical shifts of CT26 in TFE/water solution at 298 K.

Figure 3 illustrates the summary of the NOE connec-

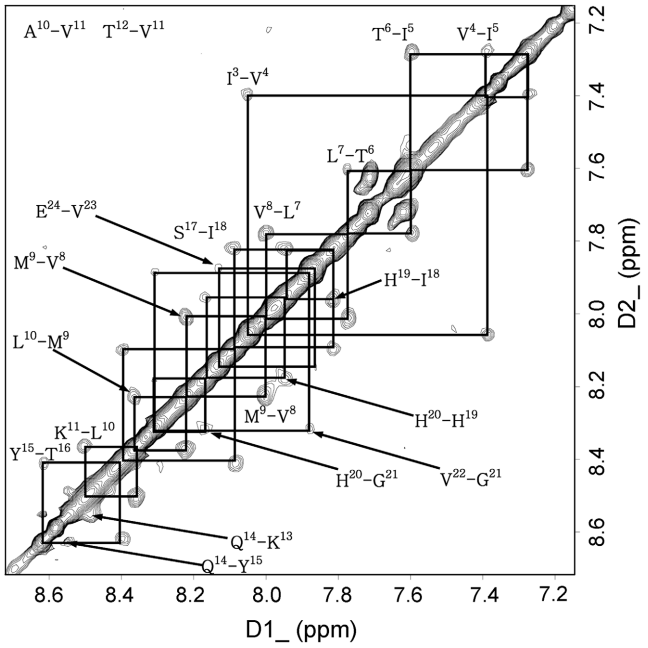

Figure 2. The NH-NH region of a 250 ms mixing time NOESY spectrum of CT26 in TFE/H_2O (1 : 1, v/v) solution at 298 K, pH 4.0.

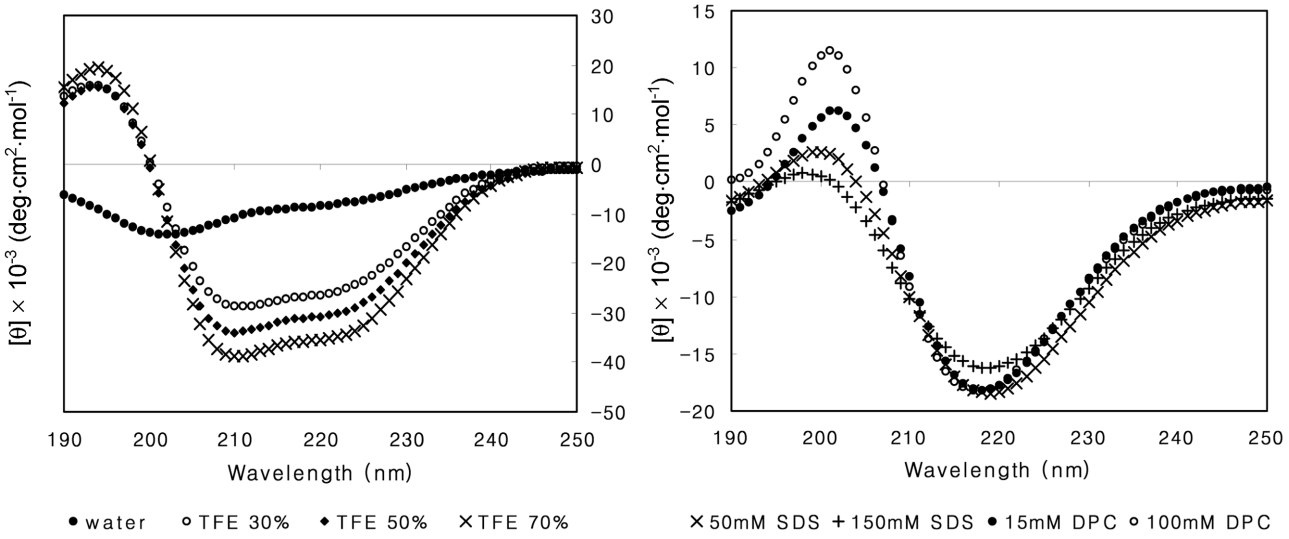

Figure 1. CD spectra of CT26 in various environments. (a) in various concentration of TFE-H_2O mixture solvents (b) in various concentration of SDS micelles and DPC micelles at 298 K.

Table 1. ^{1}H chemical shifts (ppm) for CT26 in TFE/H_2O (1 : 1, v/v) solution at 298 K, pH 4.0

Residue	*Chemical shift (ppm)*[a]			
	NH	αH	βH	Others
Thr[1]				
Val[2]	8.50	4.10	2.20	γ 1.07*
Ile[3]	8.04	4.16	1.90	γ CH_3 0.93*; γ CH_2 1.00*; γ 0.81*
Val[4]	7.37	3.87	2.13	γ 1.02, 1.07
Ile[5]	7.27	3.91	1.95	γ CH_3 0.97*; γ CH_2 1.01*; δ 0.90*
Thr[6]	7.58	4.29	3.97	γ 1.30*
Leu[7]	7.75	4.16	1.89	γ 1.64*; γ 0.75*
Val[8]	7.98	3.61	2.12	γ 0.99*
Met[9]	8.19	4.20	2.17*	γ 2.43*
Leu[10]	8.34	4.15	1.65	γ 1.60*; δ 0.85
Lys[11]	8.47	4.14	1.77*	γ 1.43*; δ 1.71*; ε 3.08*
Lys[12]	8.46	4.25	1.91*	γ 1.47*; δ 1.67*; ε 3.10*
Lys[13]	8.44	4.12	1.84*	γ 1.53; δ 1.70*; ε 3.18*
Gln[14]	8.53	4.23	2.20, 2.30	γ 2.60*
Tyr[15]	8.59	4.30	3.25*	2, 6H 7.18; 3, 5H 6.85
Thr[16]	8.37	4.18	4.04	γ 1.41*
Ser[17]	8.07	4.41	4.02, 4.08	
Ile[18]	7.79	4.07	1.80	γ CH_3 0.85*; γ CH_2 1.01*; δ 0.74*
His[19]	7.94	4.20	2.86, 2.93	2H 8.59; 4H 7.33
His[20]	8.13	4.51	3.30, 3.42	2H 8.60; 4H 7.42
Gly[21]	8.29	3.98, 4.04		
Val[22]	7.87	4.19	2.10	γ 1.00*
Val[23]	7.85	4.19	2.15	γ 0.93*
Glu[24]	8.11	4.51	2.07, 2.15	γ 2.45*
Val[25]	7.97	4.21	2.15	γ 0.97*
Asp[26]				

[a]Chemical shifts are relative to DSS (0 ppm)

tivities, $^3J_{HN}$ coupling constants and chemical shift indices in TFE/H_2O (1 : 1, v/v) solution. The observation of sequential $d_{NN}(i,i+1)$ and medium range $d_{\alpha\beta}(i,i+3)$, $d_{\alpha N}(i,i+3)$ and $d_{\alpha N}(i,i+4)$ NOEs strongly supports the presence of α-helix spanning residues from Val[2] to Lys[11] in CT26. The observed values of the $^3J_{HN\alpha}$ coupling constants for this region are generally below 6 Hz and they are marked with small size filled circle. A dense grouping of four or more −1 value of chemical shift indices not interrupted by a +1 in this region is another evidence of α-helix.[27] The presence of small $^3J_{HN\alpha}$ coupling constants, the sequence of residues with chemical shift indices of –1, and the NOE patterns present strong evidences that CT26 in TFE/H_2O (1 : 1, v/v) solution have an a-helical structure in the N-terminus.

Tertiary Structures of CT26. To determine the tertiary structure of CT26, we used experimental restraints such as sequential ($|i-j|=1$), medium-range ($1<|i-j|\leq 5$), long-range ($|i-j|>5$), intraresidual distance, and torsion angle restraints, as listed in Table 2. From the structures, which were accepted with a small deviations from idealized covalent geometry and experimental restraints (≤ 0.05 Å for bonds, ≤ 5° for angles, ≤ 5° for chirality, ≤ 0.3 Å for NOE restraints, and ≤ 3° for torsion angle restraints), and 20 output structures with the lowest energy for each peptides were analyzed (N, C_α, C', O).

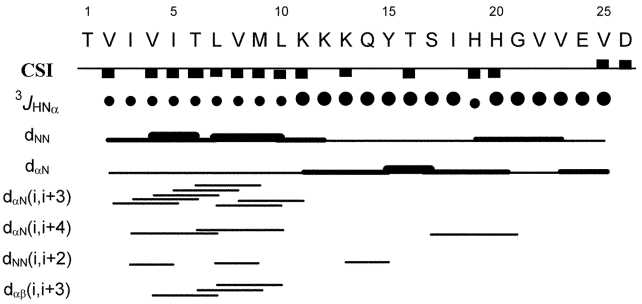

Figure 3. The NOE connectivities, $^3J_{HNa}$ coupling constants and chemical shift indices of CT26 in TFE/H_2O (1 : 1, v/v) solution at 298 K, pH 4.0. The size of filled circle is proportional to the value of measured $^3J_{HNa}$.

Table 2. Structural statistics and mean pairwise rms deviations for the 20 best structures of CT26 in TFE/H_2O (1 : 1 v/v) solution[a]

(a)	CT26
Experimental distance restraints	
Total	152
Sequential	71
Medium range	30
Intraresidue	51
H-bond (two per bond)	0
Dihedral angle restraints	24
R.m.s.d from experimental restraints	
NOE (Å)	0.017 ± 0.007
ϕ (deg)	0.016 ± 0.017
R.m.s.d from idealized covalent geometry	
Bonds (Å)	0.001 ± 0.0001
Angles (deg)	0.445 ± 0.008
Impropers (deg)	0.349 ± 0.014
Average energies (kcal mol^{-1})	
E_{tot}	31 ± 1.4
E_{NOE}	1.3 ± 0.91
E_{tor}	24.0 ± 0.85
E_{repel}	1.32 ± 0.55
(b)	
R.m.s.d from the mean structure	
Backbone atoms of all residues	3.01 ± 0.75
All heavy atoms of all residues	4.21 ± 1.11
Backbone atoms (2-11)	0.62 ± 0.20
All heavy atoms (2-11)	1.36 ± 0.27

[a]E_{NOE}, E_{tor} and E_{repel} are the energies related to the NOE violations, the torsion angle violations, and the van der Waals repulsion term, respectively. The value of the square-well NOE (E_{NOE}) and torsion angle (E_{tor}) potentials are calculated with force constants of 50 kcal mol^{-1} $Å^{-2}$ and 200 kcal mol^{-1} rad^{-2}, respectively. The values of the quartic van der Waals repulsion term (E_{repel}) is calculated with a force constant 4 kcal mol^{-1} $Å^{-4}$. The rmsd values were obtained by best fitting the backbone atom (N, Cα, C', O) coordinates for all residues of the 20 converged structures. The numbers given for the backbone and all heavy atoms represent the mean values ± standard deviations.

The statistics of the 20 final simulated annealing (SA) structures of CT26 are given in Table 2. All 20 SA structures display good covalent geometries and small NMR constraint violations. When we superimposed the 20 structures on the backbone atoms of the residues from Val[2] to Lys,[11] their rms deviations from mean structure are 0.62 Å for the backbone

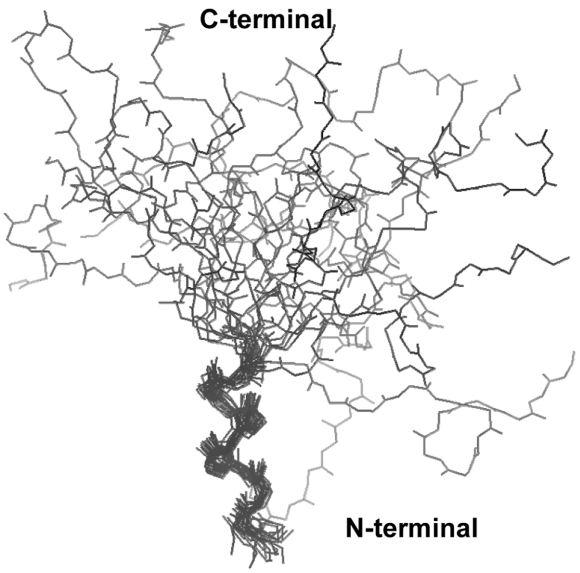

Figure 4. The superpositions of the 20 lowest energy structures of CT26 (APP639-664) calculated from the NMR data, using backbone atoms of residues 2-11.

atoms and 1.36 Å for all heavy atoms. However, the rms deviations for all residues from the mean structures are much bigger for all peptides because of the flexible region. Figure 4 shows the superposition of 20 lowest energy structures of CT26 calculated from the NMR data using backbone atoms of residue 2-11. CT26 has an α-helical structure from from Val^2 to Lys^{11} and the C-terminus shows a random structure with great flexibilities.

Conclusion

We have investigated the structure of CT26 by NMR spectroscopy and circular dichroism spectropolarimeter. The N-terminus of this peptide is generated by γ-secretase cleavage creating Aβ and the C-terminal is generated by caspase cleavage relevant to cell death. From the circular dichroism study, it was confirmed that CT26 exists as α-helix structure in TFE aqueous solution and as β-sheet structure in SDS or DPC micelle.

It has been proposed by CD spectroscopy that Aβ25-35 exhibits pH- and concentration-dependent α-helix $\leftrightarrow$ β-sheet transition and 25-35 fragment shows lipid-induced reversible random-coil $\leftrightarrow$ β-sheet transition.[28] This conformational transition with concomitant peptide aggregation can be a possible mechanism of plaque formation. We have determined the structure of Aβ25-35 in aqueous TFE solution using NMR spectroscopy and Aβ25-35 has α-helical structures in its C-terminal region and aromatic rings or hydrophobic side chains in the center of the helix protrude outside.[29]

Tertiary structure of CT26 in TFE/H_2O (1 : 1, v/v) solution determined by NMR spectroscopy shows that CT26 has α-helix spanning from Val^2 to Lys^{11}. CT26 were aggregated in both micelles at 1 mM concentration and this implies that aggregations of CT26 in SDS micelles or DPC micelle result from the β-sheet structure. Therefore, it can be proposed that CT26 exhibits environment-dependent α-helix $\leftrightarrow$ β-sheet transition like Aβ25-35 fragments. Thr^1 to Leu^{10} of CT26 is a transmembrane domain and α-helical structure of this region is likely to be related to the transmembrane action regulating the activity of CT by α-helix $\leftrightarrow$ β-sheet transition. This study may provide an insight into the conformational basis of the pathological activity of the C-terminal fragments of APP in the model membrane.

Acknowledgment. This work was supported by a Molecular and Cellular BioDiscovery Research Program grant from the Ministry of Science and Technology of Korea and, in part, by the Bio/Molecular Informatics Center in Konkuk University (KRF2004-F00019).

References

1. Suh, Y. H. *Life Science & Biotechnology* **2000**, *14*, 16.
2. Selkoe, D. J. *J. Neuropathol. Exp. Neurol.* **1994**, *53*, 438.
3. Checler, F. *J. Neurochem.* **1995**, *65*, 1431.
4. Haass, C.; Koo, E. H.; Mellon, A.; Hung, A. Y.; Selkoe, D. J. *Nature* **1992**, *357*, 500.
5. Golde, T. E.; Estus, S.; Younkin, L. H.; Selkoe, D. J.; Younkin, S. G. *Science* **1992**, *255*, 728.
6. Matsumoto, A. *Biochem. Biophys. Res. Commun.* **1994**, *175*, 361.
7. Kametani, F.; Tanaka, K.; Tokuda, T.; Ikeda, S. *FEBS Lett.* **1994**, *351*, 165.
8. Lee, S.; Kim, Y. *Bull. Korean Chem. Soc.* **2004**, *25*, 838.
9. Fukuchi, K.; Sopher, B.; Furlong, C. E.; Sundstrom, J. A.; Smith, A. C.; Martin, G. M. *Neurosci. Lett.* **1993**, *154*, 145.
10. Oster-Granite, M. L.; Greenan, J.; Neve, R. L. *J. Neurosci.* **1996**, *16*, 6732.
11. Arters, J.; Mcphie, D.; Neve, R. L.; Berger-Sweeny, J. *Soc. Neurosci. Abst.* **1995**, *21*, 1483.
12. Bertrand, E.; Brouillet, E.; Caille, I.; Bouillot, C.; Cole, G. M.; Prochiantz, A.; Allinquant, B. *Mol Cell Neurosci.* **2001**, *18*(5), 503.
13. Nishimoto, I.; Okamoto, T.; Matsuura, Y.; Takahashi, S.; Okamoto, T.; Murayama, Y.; Ogata, E. *Nature* **1993**, *362*, 75.
14. Derome, A.; Williamson, M. *J. Magn. Reson.* **1990**, *88*, 177.
15. Bax, A.; Davis, D. G. *J. Magn. Reson.* **1985**, *65*, 355.
16. Macura, S.; Ernst, R. R. *Mol. Phys.* **1980**, *41*, 95.
17. Bax, A.; Davis, D. G. *J. Magn. Reson.* **1985**, *63*, 207.
18. Marion, D.; Wüthrich, K. *Biochem. Biophys. Res. Commun.* **1983**, *113*, 967.
19. Kim, Y.; Prestegard, J. P. *J. Magn. Reson.* **1989**, *84*, 9.
20. Clore, G. M.; Gronenborn, A. M. *CRC Crit. Rev. Biochem. Mol. Biol.* **1989**, *24*, 479.
21. Clore, G. M.; Gronenborn, A. M. *Protein Sci.* **1994**, *3*, 372.
22. Brünger, A. T. *X-PLOR Manual, Version 3.1*; Yale University, New Haven, CT, 1993.
23. Wüthrich, K.; Billeter, M.; Braun, W. *J. Mol. Biol.* **1983**, *169*, 949.
24. Clore, G. M.; Gronenborn, A. M.; Nilges, M.; Ryan, C. A. *Biochemistry* **1987**, *26*, 8012.
25. Nilges, M.; Clore, G. M.; Gronenborn, A. M. *FEBS Lett.* **1988**, *229*, 317.
26. Kuszewski, J.; Nilges, M.; Brünger, A. T. *J. Biomol. NMR* **1992**, *2*, 33.
27. Wishart, D. S.; Sykes, B. D.; Richards, F. M. *Biochemistry* **1992**, *31*, 1647.
28. Symmons, M. F.; Buchanan, S. G.; Clarke, D. T.; Jones, G.; Gay, N. J. *FEBS Lett.* **1997**, *412*, 397.
29. Lee, S.; Suh, Y. H.; Kim, S.; Kim, Y. *J. Biomol. Struct. Dyn.* **1999**, *17*, 381.